Cancer Cell
Article

Discovery and Characterization of Super-Enhancer-Associated Dependencies in Diffuse Large B Cell Lymphoma

Bjoern Chapuy,[1,7] Michael R. McKeown,[1,7] Charles Y. Lin,[1] Stefano Monti,[2] Margaretha G.M. Roemer,[1] Jun Qi,[1] Peter B. Rahl,[3,9] Heather H. Sun,[4] Kelly T. Yeda,[1] John G. Doench,[5] Elaine Reichert,[1] Andrew L. Kung,[6,10] Scott J. Rodig,[4] Richard A. Young,[3] Margaret A. Shipp,[1,8,*] and James E. Bradner[1,8,*]

[1]Department of Medical Oncology, Dana-Farber Cancer Institute, Boston, MA 02115, USA
[2]Section of Computational Biomedicine, Boston University School of Medicine, Boston, MA 02118, USA
[3]Whitehead Institute of Genome Research, Massachusetts Institute of Technology, Cambridge, MA 02142, USA
[4]Department of Pathology, Brigham and Women's Hospital, Boston, MA 02115, USA
[5]Broad Institute, Cambridge, MA 02142, USA
[6]Department of Pediatric Oncology, Dana-Farber Cancer Institute, Boston, MA 02215, USA
[7]These authors contributed equally to this work
[8]These authors contributed equally to this work
[9]Present address: Syros Pharmaceuticals, Watertown, MA 02472, USA
[10]Present address: Department of Pediatrics, Columbia University, New York, NY 10032, USA
*Correspondence: margaret_shipp@dfci.harvard.edu (M.A.S.), james_bradner@dfci.harvard.edu (J.E.B.)
http://dx.doi.org/10.1016/j.ccr.2013.11.003

SUMMARY

Diffuse large B cell lymphoma (DLBCL) is a biologically heterogeneous and clinically aggressive disease. Here, we explore the role of bromodomain and extra-terminal domain (BET) proteins in DLBCL, using integrative chemical genetics and functional epigenomics. We observe highly asymmetric loading of bromodomain 4 (BRD4) at enhancers, with approximately 33% of all BRD4 localizing to enhancers at 1.6% of occupied genes. These super-enhancers prove particularly sensitive to bromodomain inhibition, explaining the selective effect of BET inhibitors on oncogenic and lineage-specific transcriptional circuits. Functional study of genes marked by super-enhancers identifies DLBCLs dependent on OCA-B and suggests a strategy for discovering unrecognized cancer dependencies. Translational studies performed on a comprehensive panel of DLBCLs establish a therapeutic rationale for evaluating BET inhibitors in this disease.

INTRODUCTION

Diffuse large B cell lymphoma (DLBCL) is the most common form of non-Hodgkin's lymphoma in adults. The majority of DLBCLs arise from antigen-exposed B cells during the germinal center (GC) reaction, a process that optimizes the affinity of antibodies for antigens (Klein and Dalla-Favera, 2008). Despite significant advances in the biological understanding of DLBCL pathogenesis, current treatment regimens include empiric combination immuno/chemotherapy at induction and relapse. Mechanistic insights guiding the development of targeted therapeutic agents are urgently needed, as relapsed and refractory disease comprise significant unmet medical needs (Gisselbrecht et al., 2010).

DLBCL exhibits significant biological heterogeneity. Gene expression profiling has allowed functional classification of tumors into distinct subgroups. Presently, DLBCL is described using two transcriptional classifications, commonly referred to as the cell of origin (COO) and the consensus clustering classification (CCC). The COO classification relates subsets of DLBCL

Significance

Although oncogenic transcription factors underlie the pathophysiology and biological heterogeneity of diffuse large B cell lymphoma (DLBCL), studies of transcriptional coactivator proteins are limited in this disease. In this chemical genetic study, we demonstrate the efficacy of bromodomain and extra-terminal domain (BET) inhibition and characterize the broad function of BET bromodomains in supporting the transcriptional growth program in all subclasses of DLBCL, including coactivation of E2F and MYC target genes. We define an asymmetry in the localization of bromodomain 4 to enhancer regions nearby oncogenic and master regulatory genes and expand the finding to a representative panel of cell lines and primary samples. This finding likely explains the specific transcriptional effect of BET inhibition, which modulates the expression of master transcription factors that control B cell fate and germinal center formation.

to specific stages of normal B cell development, assigning tumors to either a germinal center-B (GCB) or activated B cell (ABC) subtype (Lenz and Staudt, 2010). The CCC classification defines three groups of DLBCLs on the basis of transcriptional heterogeneity solely within tumors. Here, DLBCL subtypes rely on B cell receptor (BCR) survival signals and glycolysis (BCR) or BCR-independent fuel utilization and oxidative phosphorylation (OxPhos), or they exhibit an increased inflammatory and immune cell infiltrate (host response) (Caro et al., 2012; Chen et al., 2013; Monti et al., 2005). Both classifications provide insights into disease pathogenesis and suggest potential tumor cell dependencies and rational therapeutic targets.

Several genome sequencing studies of DLBCL defining the mutational landscape have revealed substantial genetic heterogeneity (Lohr et al., 2012; Morin et al., 2011; Pasqualucci et al., 2011; Zhang et al., 2013). In contrast to Burkitt lymphoma (BL), another germinal center-derived tumor characterized by a hallmark t(8;14) translocation of *MYC* into the immunoglobulin heavy- or light-chain enhancer region, DLBCLs have high genotypic diversity. These tumors exhibit multiple low-frequency copy number alterations (CNAs), additional chromosomal translocations, and over 50 recurrent somatic mutations (Lohr et al., 2012; Monti et al., 2012; Morin et al., 2011; Pasqualucci et al., 2011). In DLBCL, the underlying biological and genetic heterogeneity are associated with highly variable clinical outcomes, ranging from long-term overall survival (“cure”) to rapidly progressive disease (Monti et al., 2012).

Mechanistically, the transcriptional heterogeneity of DLBCL is conferred, in part, by pathologic activation or inactivation of lineage-specific and growth-associated master regulatory transcription factors (TFs), including NF-κB (Lenz and Staudt, 2010), BCL6 (Basso and Dalla-Favera, 2012), MYC (Slack and Gascoyne, 2011), and p53 (Monti et al., 2012), and also through upstream pathway deregulation. Recently, we demonstrated that multiple, low-frequency CNAs converge functionally to deregulate p53 and cell cycle, resulting in increased proliferation and enhanced signaling from the master regulatory transcription factor E2F1 (Monti et al., 2012). In this study, deregulated cell cycle and increased expression of E2F1 target genes were associated with inferior outcome (Monti et al., 2012). In recent studies, a newly defined subset of “double-hit” DLBCLs that overexpress MYC in association with BCL2 also have an unfavorable outcome (Hu et al., 2013; Johnson et al., 2012). Together, these findings underscore the centrality of master regulatory TFs in DLBCL.

TFs control cancer cell state by binding proximal (promoter) and distal (enhancer) regulatory elements (Lee and Young, 2013). The subsequent recruitment of multiprotein complexes leads to local remodeling of chromatin, which establishes mitotic memory, and transmission of transcriptional signals to RNA polymerase II (RNA Pol II) poised at genes associated with growth and survival (Fuda et al., 2009; Schreiber and Bernstein, 2002). Chromatin associated with TF binding sites is markedly enriched in histone proteins posttranslationally modified by lysine side-chain acetylation (Marushige, 1976). This mark biophysically facilitates opening of chromatin and recruits an emerging class of coactivators that recognize ε-acetyl lysine through a specialized recognition motif or bromodomain (Owen et al., 2000).

Among the 46 known bromodomain-containing proteins (Filippakopoulos et al., 2012), the subfamily of bromodomain and extra-terminal domain (BET) coactivators (BRD2, BRD3, and BRD4) are particularly appealing targets in DLBCL. Structurally, BET proteins possess twin amino-terminal bromodomains that facilitate binding to hyperacetylated promoter/enhancer regions (Filippakopoulos et al., 2012; Zhang et al., 2012), as well as a distal carboxy-terminal binding site for the positive transcription elongation factor (P-TEFb; Bisgrove et al., 2007). In cancer, BET bromodomains promote M to G1 cell cycle progression (Yang et al., 2008) and contribute to mitotic memory (Dey et al., 2003; Zhao et al., 2011). Collaborative research from our group and others has recently identified a role for BET bromodomains in supporting the transcription of known DLBCL oncogenes (*MYC* and *BCL2*) in studies of acute leukemia, multiple myeloma, and BL (Dawson et al., 2011; Delmore et al., 2011; Mertz et al., 2011; Ott et al., 2012; Zuber et al., 2011). Interestingly, overexpression of BRD2 from an engineered immunoglobulin heavy-chain promoter-enhancer construct caused an aggressive B cell neoplasm resembling DLBCL in mice (Greenwald et al., 2004). Together, the findings establish a compelling hypothesis that BET bromodomains serve as chromatin-associated modulators of major gene regulatory pathways in DLBCL.

In an effort to study the role of BET bromodomains in cancer, we recently developed specific inhibitors of BET transcriptional coactivator proteins (Filippakopoulos et al., 2010), including a prototypical triazolo-diazepine inhibitor of the acetyl-lysine binding site, JQ1. Here, we explore the role of BET bromodomains in oncogenic transcription by master regulatory TFs and assess BRD4 as a therapeutic target in DLBCL.

RESULTS

BET Bromodomain Inhibition Exerts Pan-Subtype Growth Arrest in DLBCL and in BL

To assess the role of BET bromodomains as cancer cell dependencies in DLBCL, we first studied the effects of four structurally dissimilar BET bromodomain inhibitors on a comprehensive panel of 34 human lymphoma cell lines (21 DLBCL, capturing all transcriptionally defined subtypes, 6 BL, and 7 Hodgkin’s lymphoma [HL]; Table S1 available online) in comparative high-throughput format. In addition to the prototypical BET inhibitor JQ1 (JQ1S) (Filippakopoulos et al., 2010), we resynthesized, characterized, and tested an analogous thienodiazepine from Mitsubishi-Tanabe Pharmaceutical (Y803, OTX015; Oncoethix), which was developed for inflammatory bowel disease (Figure S1A; Miyoshi et al., 2009), a benzodiazepine inhibitor (iBET; Nicodeme et al., 2010), and a dimethylisoxazole inhibitor (iBET-151) from GlaxoSmithKline (Dawson et al., 2011). Analyses of cellular proliferation at 72 hr revealed a potent class effect of BET bromodomain inhibitors on the DLBCL and BL cell lines irrespective of subtype and the lack of effect of an inactive enantiomer, JQ1R (Figure 1A). The HL cell lines were comparatively less sensitive to BET inhibition and one HL line, L428, was resistant to all four compounds.

The effects of BET inhibition on growth over time, cell cycle progression, and apoptosis were then studied in a representative panel of nine DLBCL cell lines, using the L428 HL line as a negative control (Figures 1B, 1C, S1B, and S1C). BET inhibition with

JQ1 significantly attenuated growth in a dose-responsive manner in all tested DLBCL cell lines (Figure 1B). In three representative DLBCL cell lines, genetic depletion of BRD2 or BRD4 similarly decreased DLBCL proliferation, consistent with an on-target effect of JQ1 (Figures S1D–S1G). We observed a profound S phase and G2 peak reduction following JQ1 treatment, consistent with a G1 cell cycle arrest (Figures 1C and S1B). BET inhibition (500 nM) did not induce apoptosis in most cell lines studied, evidenced by low AnnexinV/7AAD staining (Figure S1C) and absence of a sub-G1 peak (Figure 1C). Neither enantiomeric (JQ1R) nor vehicle (DMSO) controls affected DLBCL proliferation or survival (Figures 1C, S1B, and S1C). Treatment with 500 nM JQ1 was similarly cytostatic in BL cell lines (Figure S1C). The L428 HL cell line was resistant to BET inhibition in all tested assays.

Efficacy of BET Inhibition in DLBCL Xenograft Models

We next explored the therapeutic potential of BET inhibition in two independent DLBCL xenotransplantation models (Figures 1D–1G and S1H–S1K). First, the human DLBCL cell line Ly1 was engineered to ectopically express firefly luciferase and mCherry, allowing surrogate measurement of tumor growth in vivo. Nonobese diabetic severe combined immunodeficiency IL2Rγ^{null} (NSG) mice xenotransplanted with Ly1-Luc-mCherry cells had a statistically significant reduction in tumor burden when treated with JQ1 (30 mg twice daily by intraperitoneal [IP] injection; Figure 1D). A representative cohort of animals was sacrificed on day 13 of treatment for full hematological analysis. JQ1-treated animals had significantly decreased lymphoma infiltration of the bone marrow (BM) as measured by flow cytometric assessment of mCherry$^+$ cells (Figure 1E). Morphological and immunohistochemical analyses revealed that the highly proliferative (Ki67$^+$) human CD20$^+$ lymphoma cell infiltrate (Figure 1F, upper panel) was markedly reduced in animals treated with the BET bromodomain inhibitor (Figure 1F, lower panel). In the remainder of the Ly1 xenograft cohort, the JQ1-treated mice had a significant median overall survival advantage of 9 days ($p = 0.003$; Figure 1G).

To confirm the pharmacodynamic findings, a second xenotransplantation model was established using the Toledo DLBCL cell line. NSG mice with established tumors had delayed tumor progression when treated with JQ1 (Figure S1H). Full hematological analysis revealed that JQ1-treated animals had lower spleen weights (Figure S1I) and decreased lymphomatous infiltration of bone marrow and spleen (Figure S1J). Morphological and immunohistochemical analysis of the BM revealed significantly reduced the infiltration of CD20$^+$/Ki67$^+$ human lymphoma cells following BET inhibition (Figure S1K).

BET Inhibition Downregulates Oncogenic Transcriptional Pathways

To gain insights into the transcriptional pathways regulated by BET bromodomain coactivator proteins, we performed kinetic transcriptional profiling of vehicle- and JQ1-treated DLBCL cell lines. Five human DLBCL cell lines that captured the recognized transcriptional heterogeneity (Ly1, BCR/GCB; DHL6, BCR/GCB; Ly4, OxPhos/unclassified; Toledo, OxPhos/unclassified; and HBL1, BCR/ABC) were treated with JQ1 (500 nM) or vehicle control for 0, 2, 6, 12, 24, and 48 hr. At each time point, differential analysis was performed between the vehicle- and JQ1-treated samples (24 hr comparison, fold change (FC) > 1.3, false discovery rate (FDR) < 0.01; Figure S2A). Consistent with prior studies of BET bromodomain function and inhibition, HEXIM1 was markedly upregulated by JQ1 in all DLBCL cell lines (Figure S2B; Bartholomeeusen et al., 2012; Puissant et al., 2013).

The most differentially expressed genes were assessed for pathway enrichment using a comprehensive pathway compendium (C2, CP; MSigDB 3.0), and each time point was ranked by FDR and visualized as a color-coded matrix (Figure 2A; full list in Table S2). We observed the early downregulation of MYD88/toll-like receptor (TLR) pathway components following JQ1 treatment, including TLR10 and MYD88 (Figures 2A–2C and S2C). These data are consistent with previous studies in which the anti-inflammatory effect of BET inhibition in normal B cells was attributed to TLR pathway downregulation (Nicodeme et al., 2010). In the JQ1-treated DLBCL cell lines, we also observed downregulation of multiple components of the BCR signaling pathway, E2F transcriptional targets, and additional cell cycle transition gene sets (Figures 2A and S2D). Similar results were obtained when GCB and ABC DLBCL cell lines were analyzed separately (Figures S2E and S2F).

BET Inhibition Modulates MYC and E2F Target Gene Transcription

Cell state transitions are influenced by the function of specific regulatory TFs. To identify candidate TFs associated with BET bromodomain coactivators, we assessed the effects of JQ1 on sets of genes with common TF binding motifs (C3; MSigDB 3.0). The differentially expressed genes in vehicle- versus JQ1-treated DLBCL cell lines were tested for enrichment of candidate TF targets at 2–48 hr. Results at each time point were ranked by FDR and visualized as a color-coded matrix (Figure 2D; Table S2).

It is of interest that gene sets with MYC and E2F binding motifs were significantly downregulated following JQ1 treatment (Figure 2D). To further evaluate the effects of BET bromodomain inhibition on MYC and E2F transcriptional programs, we used multiple functionally validated MYC and E2F target gene sets to perform directed pathway analyses. Following JQ1 treatment, there was highly significant early downregulation of well-defined and functionally validated MYC and E2F target gene sets (Figures 2E, 2F, S2G, and S2H). In complementary studies, we performed gene set enrichment analyses (GSEA) of multiple independent MYC and E2F target gene sets in vehicle- versus JQ1-treated samples and found that MYC and E2F targets were significantly less abundant in JQ1-treated cells (Figures 2F, S2I, and S2J).

BET bromodomain proteins may function as coactivators of the MYC and E2F proteins and/or as direct modulators of MYC and E2F expression. To distinguish between these possibilities, we assessed the transcript abundance and protein levels of MYC and E2F in vehicle- and JQ1-treated DLBCLs. BET bromodomain inhibition resulted in an apparent decrease in MYC transcripts and protein in each of the DLBCL cell lines (Figures 2G, S2K, and S2L), suggesting that BET bromodomains directly modulate MYC transcription. The consequences of MYC downregulation following BET inhibition have been characterized by our group and others in hematologic malignancies

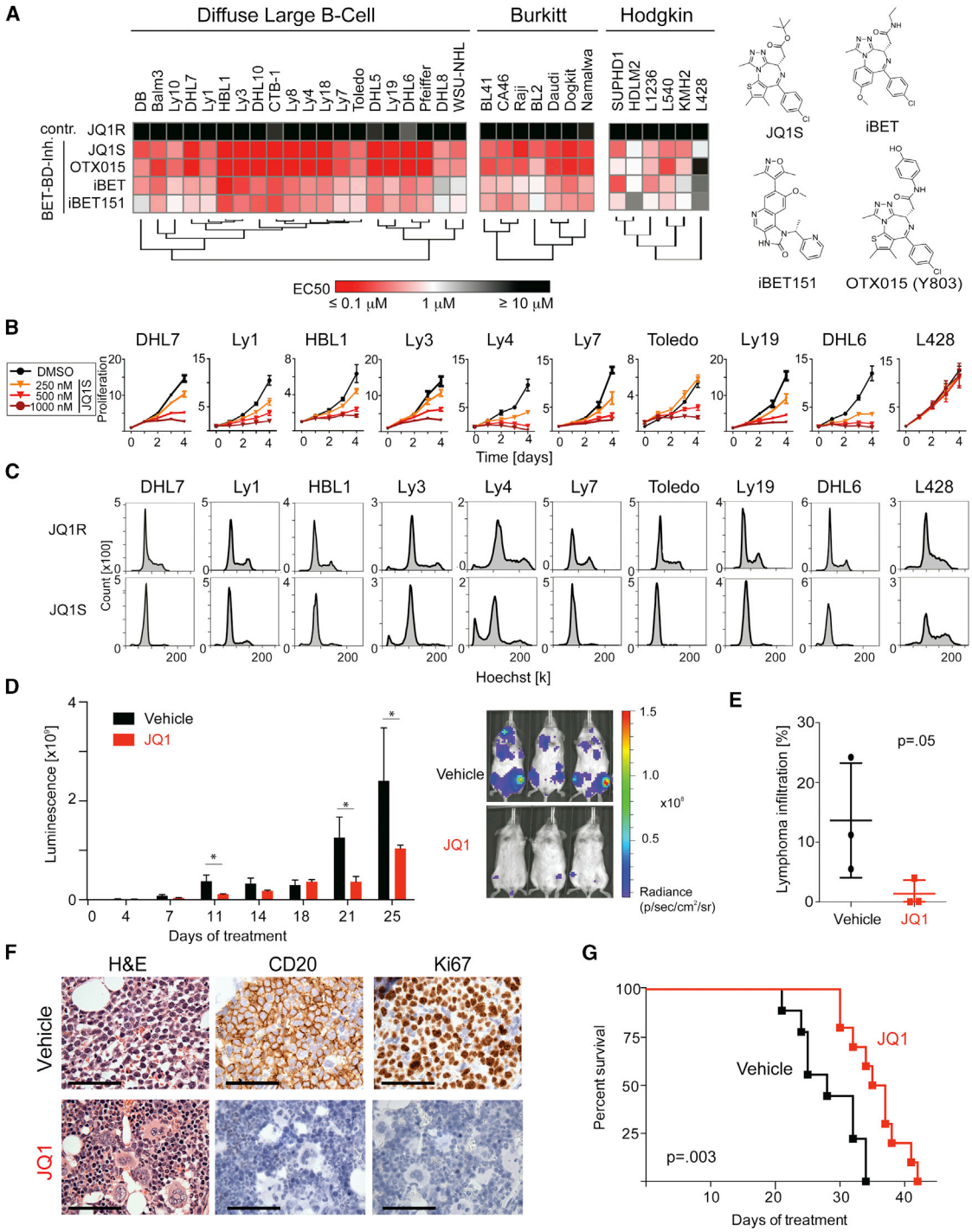

Figure 1. In Vitro Analyses of BET Bromodomain Inhibition in Various B Cell Lymphomas

(A) Hierarchical clustering of mean EC_{50}s of the four BET inhibitors (72 hr treatment) in the indicated panel of B cell lymphoma cell lines. EC_{50} values in a colorimetric scale: very sensitive ($\leq$1 μM) in red, sensitive (=1 μM) in white, to resistant ($\geq$10 μM) in black. Corresponding structures are shown.

(B) Proliferation of the indicated DLBCL and HL cell lines treated with vehicle or 250-1000 nM JQ1 for 1-4 days.

(C) Cell cycle analysis following 72 hr treatment with JQ1 (500 nM) or inactive enantiomer JQ1R (500 nM). Error bars represent the SD of triplicates.

(D) Bioluminescence of JQ1 (30 mg/kg IP twice daily) or vehicle-treated NSG mice xenotransplanted with luciferized mCherry$^+$ Ly1 cells. Asterisks indicate $p < 0.05$ using a one-sided t test. Error bars represent SEM.

(E) Lymphoma infiltration of BM in a representative set of animals was assessed by flow cytometric analysis of mCherry+ cells and visualized as scatter plots (median, line; whiskers, SEM). The p values were obtained with a one-sided Mann-Whitney U test.

(legend continued on next page)

(Dawson et al., 2011; Delmore et al., 2011; Mertz et al., 2011; Zuber et al., 2011). Notably, ectopic expression of MYC in DLBCL cell lines failed to rescue the antiproliferative effects of JQ1 (Figures S2M–S2O), also consistent with a model in which BET bromodomains function as coactivators of MYC target gene transcription. In contrast to effects on MYC expression, in four of five cell lines, JQ1 treatment did not measurably alter E2F1 transcript or protein abundance over 24 hr (Figures 2G, S2P, and S2Q). These data suggest that BET bromodomains may function at regulatory elements at E2F1 target genes, rather than by influencing the abundance of E2F1 itself.

BET Bromodomains as Promoter-Bound Coactivators of E2F1-Dependent Transcription

To explore the role of BETs as coactivators of oncogenic E2F1 transcriptional signaling, we performed chromatin immunoprecipitation with massively parallel sequencing (ChIP-seq), using a chemical genetic approach. We selected Ly1 cells for mechanistic consideration owing to the robust downregulation of E2F target genes in the transcriptional profiling (Figure S3A) and the lack of effect of JQ1 on E2F1 protein expression (Figure 2G). Changes in BET localization, chromatin structure, and RNA polymerase function were studied in Ly1 cells treated with JQ1 (500 nM) or vehicle control.

First, we established a chromatin landscape for Ly1 using H3K4me3 to identify promoters, H3K27ac to reveal enhancers, and H3K27me3 to define repressive regions of the genome. Then, we assessed the genome-wide localization of E2F1 and the representative BET protein, BRD4, also by ChIP-seq using the respective antibodies. Rank ordering of all transcriptionally active promoters based on H3K4me3 enrichment and RNA Pol II occupancy identifies pervasive binding of BRD4 and E2F1 to active promoter elements (Figure 3A). Analysis of enrichment data as a metagene of all active promoters centered on the transcription start site reveals spatial colocalization of E2F1 and BRD4 at all transcriptionally active promoters (Figure 3B).

ChIP-seq for E2F1 allowed the annotation of an E2F1 target gene set, based on the top promoter-bound genes in Ly1 cells (Table S3). Using a gene set of the top 100 ChIP-seq-defined E2F1 targets (Table S3), we performed GSEA in Ly1 and additional DLBCL cell lines DHL6, Ly4, Toledo, and HBL1. JQ1 treatment significantly decreased the transcript abundance of our functionally defined E2F1 targets at 24 hr and 48 hr in all cell lines studied (Figures 3C and S3A). The E2F1 dependency of these DLBCL cell lines as previously reported (Monti et al., 2012) was validated herein by genetic depletion in three representative cell lines (Figures 3D, 3E, S3B, and S3C). Together, these data mechanistically establish BET bromodomains as E2F1 coactivators in DLBCL.

Disproportionate Binding of BRD4 to Overloaded Enhancers

At the time this research was initiated, studies of BET bromodomains mainly focused on effects at promoter regions of the genome. Our research in multiple myeloma identified a role for BRD4 in enforcing MYC transcription from the translocated immunoglobulin H (IgH) enhancer locus (Delmore et al., 2011), where massive accumulation of BRD4 was identified by ChIP (approximately 200-fold enrichment). As oncogenic TFs may signal to RNA Pol II through distal enhancer elements, we sought to characterize the genome-wide localization of BRD4 to enhancers in DLBCL.

Rank ordering of enhancer regions by H3K27ac enrichment reveals that BRD4 binds to the vast majority of active enhancers in the Ly1 DLBCL genome (Figure 4A, blue and red tracks). Given the established role of BCL6 in the pathogenesis of DLBCL, we also documented genome-wide colocalization of BRD4 and BCL6 at H3K27ac-defined enhancers (Figure 4A, orange tracks). A metagene for active enhancers illustrates focal, superimposable enrichment for BRD4 with H3K27ac (Figure 4B). The correlation between BRD4 occupancy and H3K27 acetylation is extremely strong genome wide, with 79.1% of H3K27ac regions containing BRD4 and 92.2% of all chromatin-bound BRD4 occurring in regions marked by H3K27ac (Figure 4C). Genome-wide binding data for BRD4 reveal that BRD4 is most commonly associated with enhancer regions, defined by the presence of H3K27ac and absence of H3K4me3 (Figure 4D).

As predicted, BRD4 load is asymmetrically distributed throughout the genome at enhancer sites. Completely unexpected is the magnitude by which BRD4 load varies among active enhancer regions (Figure 4E). Only a small subset of BRD-loaded enhancers, 285/18,330 (1.6%), account for 32% of all of the BRD4 enhancer binding in the cell (Figure 4E; Table S4). The BRD4-loaded enhancers in the Ly1 DLBCL cell line are considerably larger than typical enhancer elements, resembling the super-enhancers (SEs) we recently described with Richard Young (Lovén et al., 2013).

Notably, the top two gene loci with BRD4-loaded enhancers, *POU2AF1* (which encodes the OCA-B transcriptional coactivator protein) and *BCL6,* and additional genes with disproportionally BRD4-loaded enhancers such as *PAX5* and *IRF8* (Figure 4E), are essential for B cell fate determination and germinal center formation (Basso and Dalla-Favera, 2012; Klein and Dalla-Favera, 2008; Teitell, 2003; Wang et al., 2008). In fact, mice with genetic ablation of *POU2AF1*, *BCL6*, *PAX5*, or *IRF8* lack the ability to form germinal centers, the physiological structures from which most DLBCLs arise (Cobaleda et al., 2007; Nutt et al., 2011; Teitell, 2003; Wang et al., 2008; Ye et al., 1997). Additionally, BRD4-superloaded enhancers are found adjacent to known oncogenes relevant to DLBCL biology, such as *CD79B* and *MYC* (Figures S4A and S4B).

These data indicate that BRD4 is predominantly an enhancer-associated factor, which distributes throughout DLBCL euchromatin in a highly asymmetric manner, adjacent to known oncogenes and lineage-specific transcription factors (Figure 4E). BET bromodomain inhibition selectively decreased the transcript abundance of the 285 genes with the most BRD4-loaded SEs, in contrast to the 285 genes with the least BRD4-loaded

(F) Immunohistochemical analysis of lymphoma (Ly1) BM infiltration in JQ1- and vehicle-treated mice: hematoxylin and eosin (H&E), anti-human CD20, and anti-Ki67 immunostaining. Scale bar represents 100 μm.
(G) Kaplan-Meier plot of the remainder of the Ly1 cohort (n = 21) treated with either vehicle or JQ1 30 mg/kg twice daily. The p value was obtained by log rank test. See also Figure S1 and Table S1.

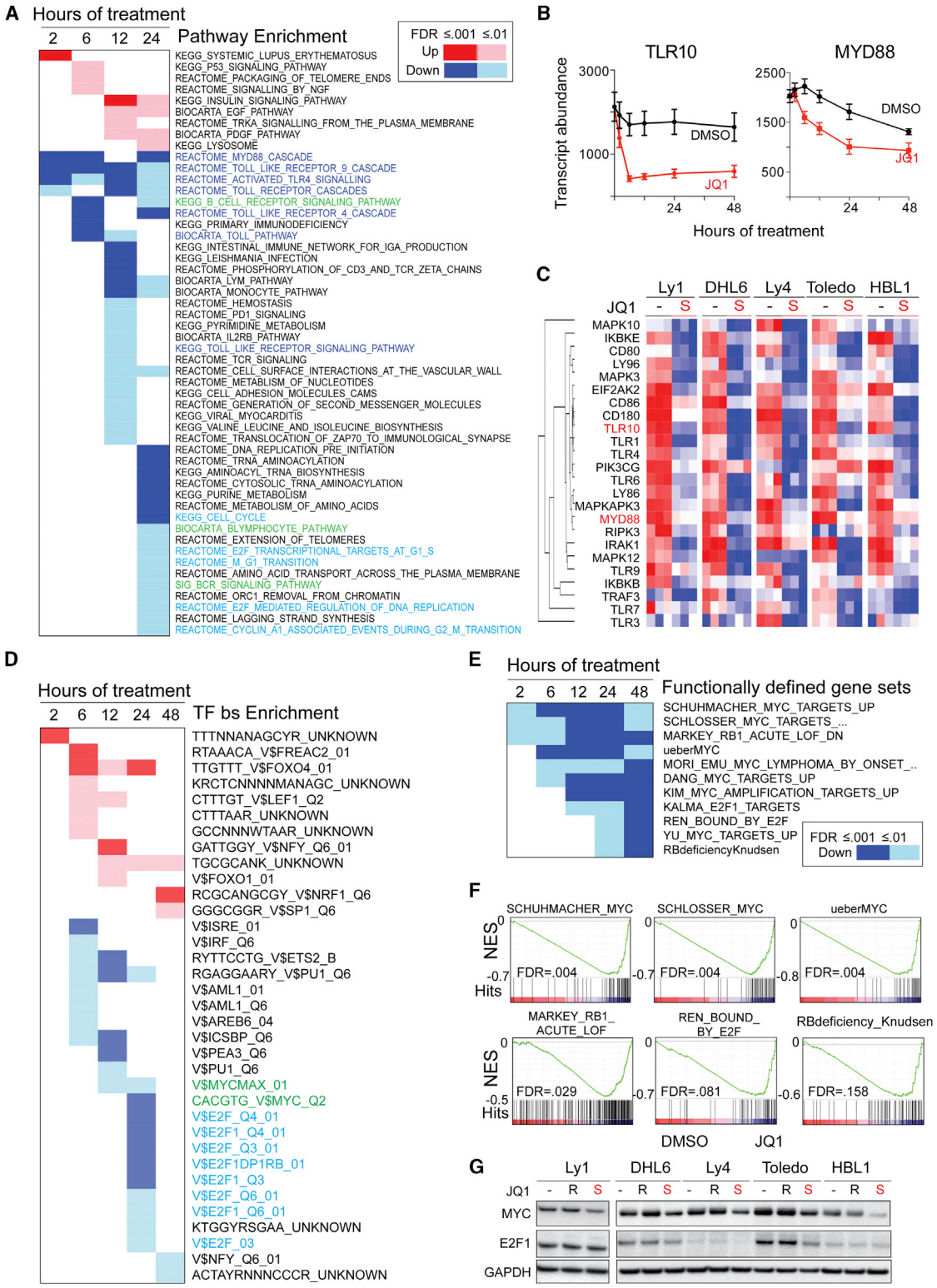

Figure 2. Transcriptional Response to BET Inhibition in Representative DLBCL Cell Lines

(A) Hyperenrichment analysis of differentially expressed genes in all five lines (FDR < 0.01; FC > 1.3) following 24 hr of treatment with 500 nM JQ1 or vehicle was performed using a pathway compendium (MSigDB, C2.CP). Results at each time point were ranked by FDR and visualized as a color-coded matrix. Upregulated pathways are in red, and downregulated pathways are in blue. Intensity of color correlates with FDR significance level. Highlighted pathways include: TLR/MYD88, blue; BCR signaling, green; and cell cycle/E2F, cyan.

(legend continued on next page)

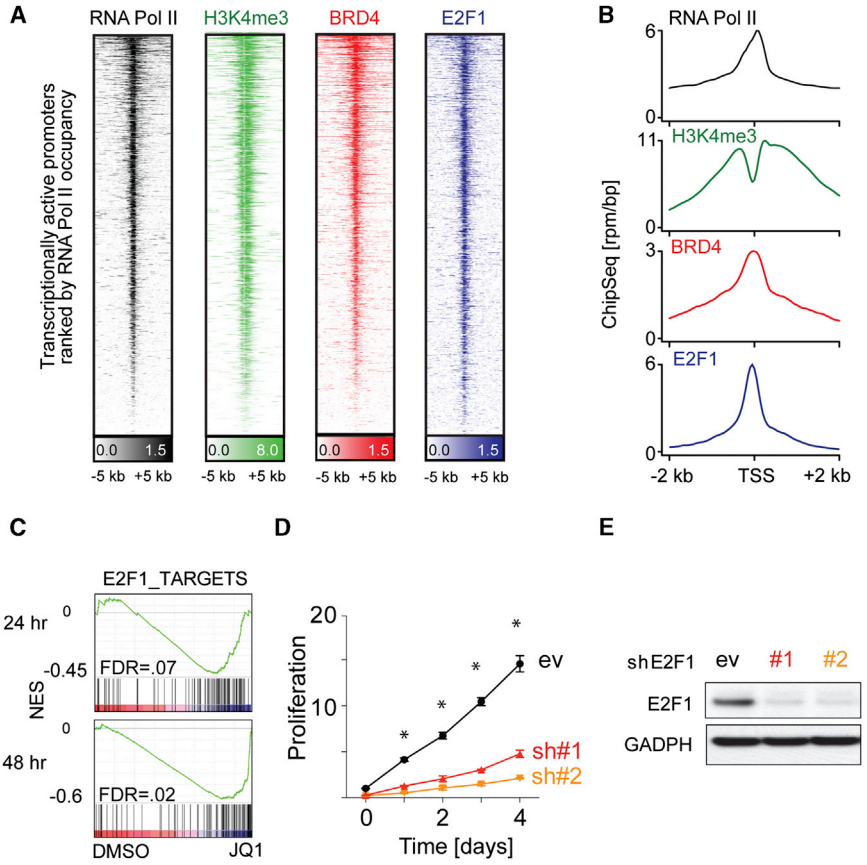

Figure 3. Colocalization and Function of BRD4 and E2F1 at Active Promoters

(A) Heatmap of ChIP-seq reads for RNA Pol II (transcriptionally active; black), H3K4me3 (green), BRD4 (red), and E2F1 (blue) rank ordered from high to low RNA Pol II occupancy centered on a ±5 kb window around the TSS of all transcriptionally active promoters. Color density reflects enrichment; white indicates no enrichment.

(B) Metagenes created from normalized genome-wide average of reads for designated factors centered on a ±2 kb window around the TSS.

(C) GSEA plots of a ChIP-seq-defined E2F1 target gene set in the five DLBCL cell lines treated with vehicle versus JQ1 for 24 and 48 hr.

(D) Assessment of proliferation in Ly1 cell line following genetic depletion of E2F1 with two independent hairpins and a control hairpin (ev). Error bars represent SD, and asterisks show $p < 0.01$ by a two-sided Student's t test.

(E) Immunoblot of E2F1 of cells in (D) to demonstrate knockdown efficiency.

See also Figure S3 and Table S3.

enhancers (Figure 4F). Similar results were obtained using H3K27ac as surrogate enhancer mark (Figure S4C). Taken together, these data suggest that BRD4 loading of select DLBCL enhancers underlies the pathway-specific transcriptional consequences of BET inhibition.

JQ1 Targets the *POU2AF1* SE and Decreases OCA-B Expression and Activity

The *POU2AF1* locus emerged as the most BRD4-overloaded enhancer in the Ly1 DLBCL cell line (Figure 4E), prompting further analysis of the effect of BET inhibition on OCA-B expression and function. OCA-B is a gene regulatory factor that interacts with the OCT1 and OCT2 TFs at octamer motifs and regulates B cell development, maturation, and GC formation (Teitell, 2003). Although OCA-B is expressed throughout B cell development, it is most abundant in normal GCB cells and GC-derived tumors, including DLBCL (Greiner et al., 2000).

POU2AF1 has a large H3K27ac-defined enhancer with strong BRD4 binding that is abolished by JQ1 treatment (Figure 5A). Consistent with this observation, BET inhibition reduced RNA Pol II elongation of *POU2AF1*, with a relative increase in promoter-paused RNA Pol II near the transcriptional start site (TSS; Figure 5B). Notably, intronic enrichment for H3K4me3 and RNA Pol II was observed in *POU2AF1*, consistent with an alternate promoter element, which was also affected by JQ1 treatment. JQ1 treatment (500 nM) decreased OCA-B transcript abundance and protein expression in Ly1 (Figure 5C), as well as additional DLBCL cell lines (Figure S5A).

We next assessed the consequences of JQ1 treatment on the OCA-B transcriptional program by performing GSEA with a well-defined series of OCA-B target genes (Table S5, modified from Teitell, 2003). OCA-B targets were downregulated in JQ1-treated DLBCLs as illustrated in Ly1 (Figure 5D) and recapitulated in the full DLBCL panel (Figures S5B and S5C). OCA-B depletion with two independent small hairpin RNAs (shRNAs) significantly decreased the proliferation of Ly1 (Figure 5E), and enforced expression of OCA-B partially rescued the JQ1-mediated antiproliferative effects (Figures S5D and S5E). Genetic depletion of either BRD2 or BRD4 phenocopied the JQ1-mediated reduction of OCA-B (Figures 5F, 5G, S5F, and S5G).

(B) Mean transcript abundance of TLR10 (left) and MYD88 (right) in all five lines. Error bars represent SEM.

(C) Heatmap of TLR pathway components in vehicle- or JQ1-treated DLBCLs (all five lines; 24 hr).

(D) The most differentially expressed genes (FDR < 0.01; FC > 1.3) were analyzed for common TF binding sites in the regulatory region using the MSigDB.C3 compendium. Results at each time point were ranked using a color-coded matrix as in (A). Genes with MYC binding sites are in green and E2F binding sites are in cyan.

(E) GSEA of multiple functionally defined MYC and E2F TF target gene sets was performed. Results are reported over time in a color-coded matrix with color intensity reflecting significance level.

(F) GSEA plots of functionally defined MYC and E2F target gene sets in vehicle- versus JQ1-treated cells at 24 hr.

(G) Protein abundance of MYC and E2F in the indicated DLBCL lines treated with vehicle or JQ1S or JQ1R (500 nM; 24 hr).

See also Figure S2 and Table S2.

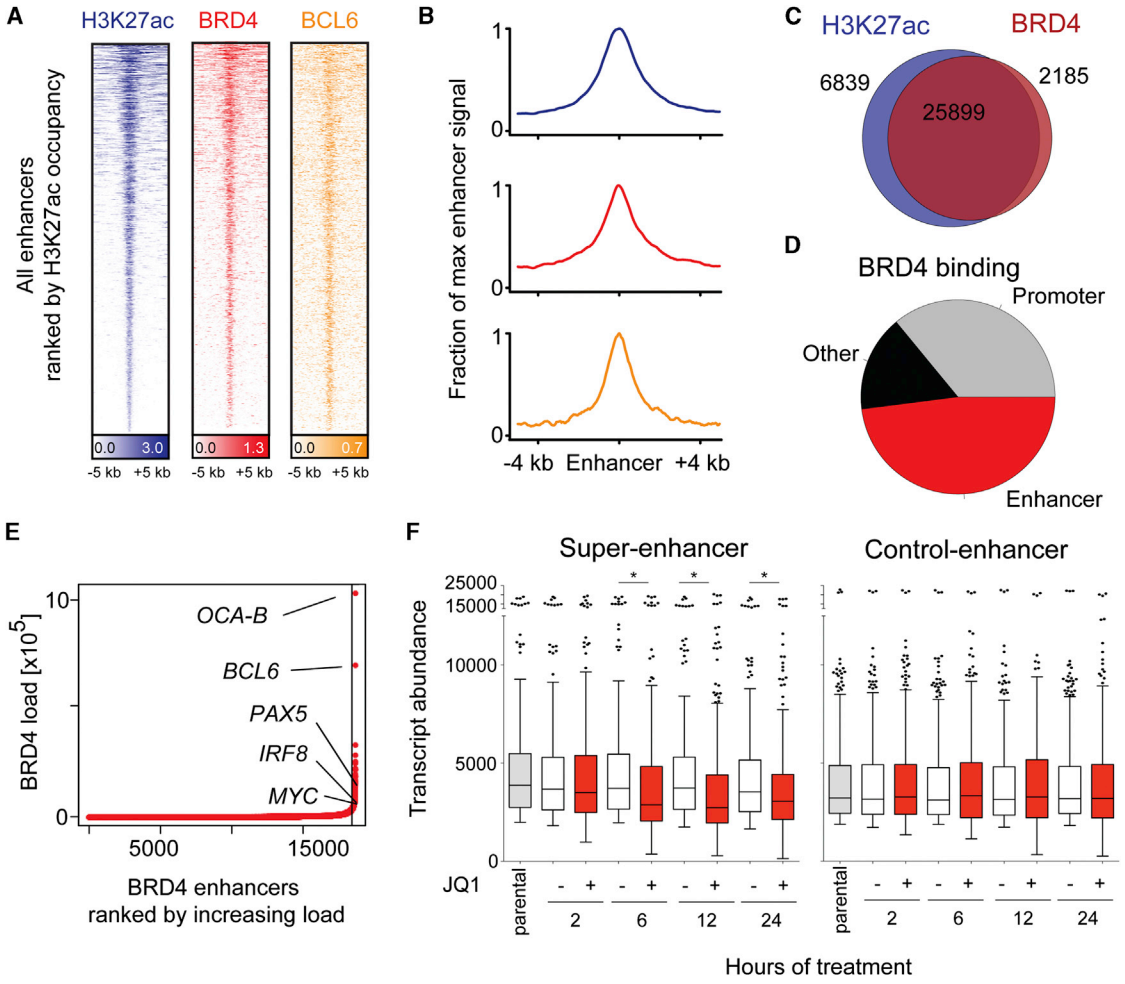

Figure 4. Asymmetric BRD4 Loading at Enhancer Elements of Actively Transcribed Genes

(A) Heatmap of ChIP-seq binding for H3K27ac (blue), BRD4 (red), and BCL6 (orange) rank ordered from high to low H3K27 occupancy centered on a ±5 kb window around enhancers. Color density reflects enrichment; white indicates no enrichment.

(B) Metagenes created from normalized genome-wide average of reads for designated factors centered on a ±4 kb window around the enhancers.

(C) Venn diagram of BRD4 binding and H3K27ac occupancy. A total of 79.1% of H3K27ac regions contain BRD4, and 92.2% of all chromatin-bound BRD4 occurs within H3K27ac regions.

(D) Pie chart of BRD4 binding to regions of the genome. BRD4 colocalization with H3K27ac without H3K4me3 defined as enhancer-bound (red); BRD4 colocalization with H3K4me3 reported as promoter-bound (gray); and remaining genomic regions in "other" (black).

(E) BRD4 loading/binding across enhancers of 18,330 genes. A total of 1.6% (285/18,330) of enhancers contain 32% of all enhancer-bound BRD4, with super-loading defined as surpassing the inflection point. Top BRD4-superloaded enhancers are indicated.

(F) Mean transcript abundance of the genes associated with the 285 most and least BRD4-loaded enhancers (left and right panel, respectively) in five DLBCL cell lines treated with vehicle or JQ1 (2–24 hr). Asterisks indicate a $p < 0.0001$ obtained using a two-sided Mann-Whitney U test.

See also Table S4 and Figure S4.

Together, these data underscore the importance of OCA-B to DLBCL growth and illustrate the use of SEs to identify cancer dependencies.

JQ1 Targets SEs of Additional Critical B Cell TFs and Modulates the GC Program

Three of the master regulatory TFs with BRD4-loaded SEs (*BCL6, IRF8*, and *PAX5*) promote and maintain the B cell gene expression program and limit differentiation into antibody-secreting plasma cells (Nutt et al., 2011). For these reasons, we further assessed the functional consequences of BET inhibition on the critical B cell TFs with BRD4-loaded SEs.

Given the known oncogenic function of deregulated BCL6 in GC B cells (Basso and Dalla-Favera, 2012) and the sensitivity of certain DLBCLs to BCL6 depletion (Polo et al., 2007), we first evaluated the consequences of BET inhibition on BCL6 expression and function. The *BCL6* locus includes a large previously defined upstream enhancer (Ramachandrareddy et al., 2010) that is severely depleted of BRD4 upon JQ1 treatment (Figure 6A). Consistent with depletion of BRD4 from the *BCL6* enhancer, the promoter reveals a suggestion of increased RNA Pol II pausing and reduced elongating RNA Pol II (Figure 6B). JQ1 treatment markedly decreased *BCL6* transcript abundance and protein expression in Ly1 (Figures 6C and 6D) and additional

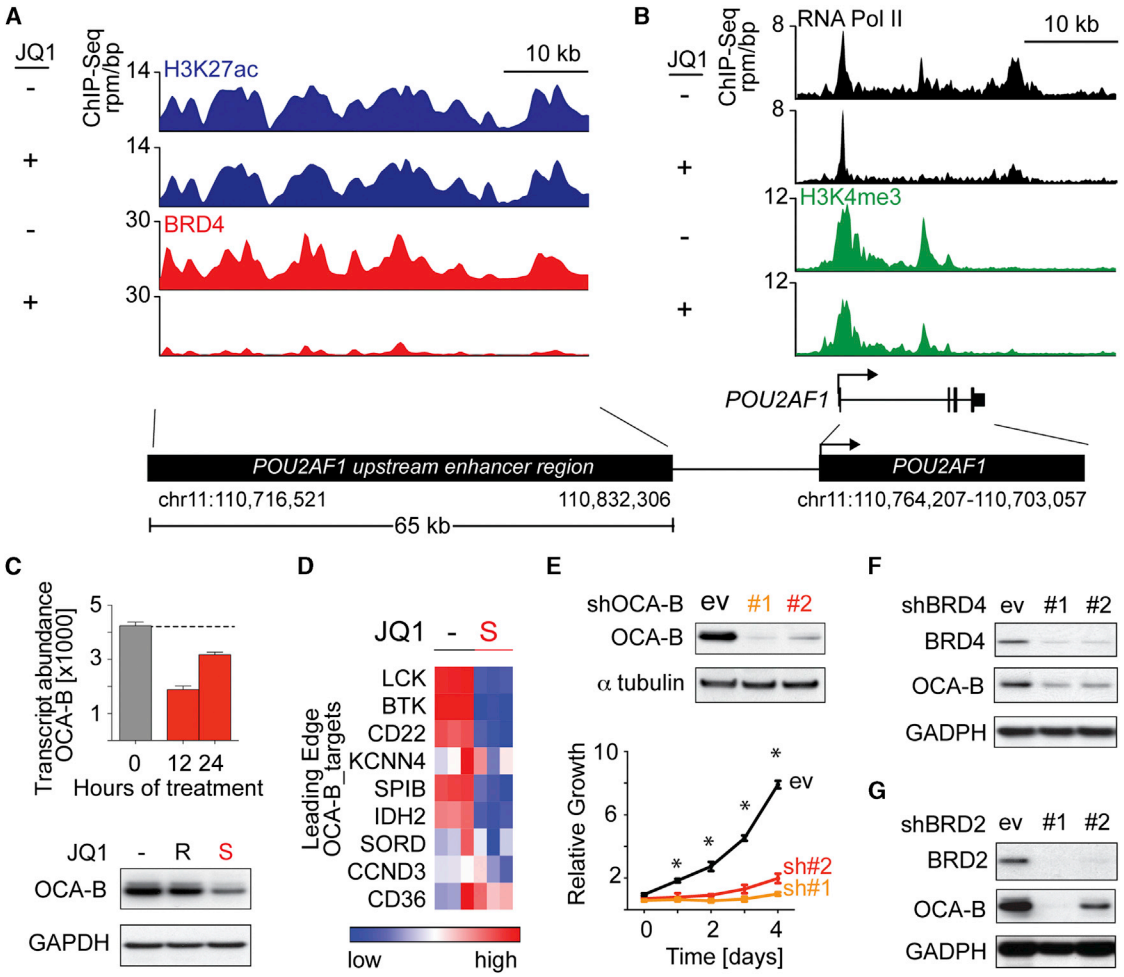

Figure 5. Identification of OCA-B as a DLBCL Dependency by SE Analysis

(A) ChIP-seq binding density for H3K27ac (blue) and BRD4 (red) at the enhancer of *POU2AF1* following JQ1 (+) or vehicle (DMSO; –) treatment.

(B) ChIP-seq reads at the *POU2AF1* promoter for RNA Pol II (black) and H3K4me3 (green) following JQ1 (+) or vehicle (–) treatment.

(C) OCA-B transcript and protein abundance in Ly1 cells treated with vehicle or 500 nM JQ1 or JQ1R (24 hr). Error bars represent SD.

(D) OCA-B target genes (leading edge, OCA-B GSEA) in Ly1 cells treated with vehicle or 500 nM JQ1 are visualized as heatmap.

(E) Knockdown efficacy of two independent OCA-B shRNAs was detected by western blot (top panel). Proliferation of OCA-B-depleted cells was measured by alamar blue. The p values for control versus each OCA-B shRNA were delineated by two-sided Student's t test; asterisks show $p < 0.01$. Error bars represent SD.

(F and G) Knockdown efficiency of two independent shRNAs against BRD4 (F) or BRD2 (G) and the associated changes in OCA-B expression were evaluated by western blot.

See also Figure S5 and Table S5.

DLBCL lines (Figure S6A). Interestingly, the observed broad localization of BCL6 to its enhancer region was reduced by JQ1 (Figures 6A and 6B), a finding we confirmed by ChIP-quantitative PCR (Figure S6B). This may reflect an influence of BET inhibition on TF binding or a consequence of downregulation of BCL6 by JQ1. Similarly, *PAX5* and *IRF8* also have BRD4-loaded SEs that are severely depleted of BRD4 following JQ1 treatment (Figure 6E). BET inhibition also decreased PAX5 and IRF8 transcript abundance and protein expression (Figures 6F and 6G).

SE Clustering Identifies Transcriptional Subtypes of DLBCL

Using the robust H3K27ac mark to identify and discriminate SEs, we conducted ChIP-seq SE analysis on five additional human DLBCL lines (DHL6, BCR/GCB; HBL1 and Ly3, BCR/ABC; Toledo and Ly4, OxPhos/unclassified; Table S7) and a normal lymphoid sample (tonsil; Table S7). Asymmetric enhancer loading was detected in all of the DLBCL cell lines (Figures 7A–7C) and the normal tonsil (Figure 7D), confirming the ubiquitous nature of this epigenomic structural element.

In all of the DLBCL cell lines and normal tonsil, large SEs were identified adjacent to genes encoding master TFs such as PAX5, OCA-B, and IRF8 (Figures 7A–7F, tracks; Table S7) that maintain the B cell program and limit plasma cell differentiation. Given the critical role of these master regulatory TFs in maintaining GC integrity and limiting GC exit (Nutt et al., 2011), we functionally assessed the consequences of BET inhibition on the GC program in all DLBCL cell lines. To that end, we

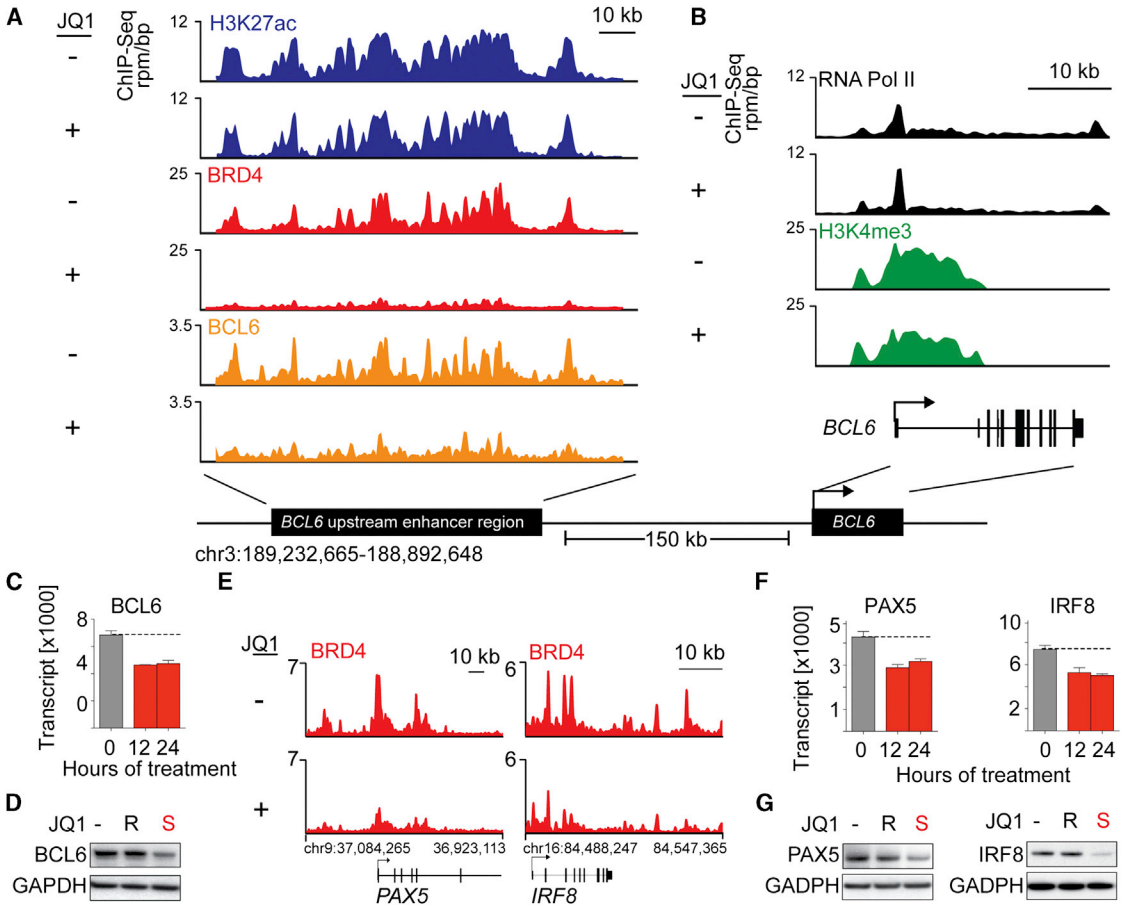

Figure 6. BET Inhibition Modulates Tissue-Specifying TF Expression by Disrupting SEs

(A) ChIP-seq binding density for H3K27ac (blue), BRD4 (red), and BCL6 (orange) at the *BCL6* enhancer following JQ1 (+) or vehicle (DMSO; −) treatment.

(B) ChIP-seq reads at the *BCL6* promoter for RNA Pol II (black) and H3K4me3 (green) following JQ1 (+) or vehicle (−) treatment.

(C) BCL6 transcript abundance in Ly1 cells 12 and 24 hr following vehicle or JQ1 treatment (derived from GEP data). Error bars represent SD.

(D) BCL6 protein abundance following treatment with vehicle or JQ1 or JQ1R (500 nM; 24 hr).

(E) ChIP-seq density of BRD4 (red) at SEs of the two additional B cell TFs, *PAX5* and *IRF8*, following treatment with JQ1 (+) or DMSO (−).

(F and G) PAX5 and IRF8 transcript (F) and protein abundance (G) in Ly1 cells following JQ1 treatment. Error bars represent SD.

See also Table S6, Figure S6, and Supplemental Experimental Procedures.

used publicly available gene expression profiles (GEP) of highly purified human B cell subsets and defined a set of genes that are significantly more abundant in GC centrocytes and centroblasts than in post-GC plasma cells (UP_IN_GCB_VS_PC). Using GSEA, we confirmed that this common GC developmental program was downregulated in Ly1 and in all five DLBCL cell lines following JQ1 treatment (Figures 7G, 7H, and S7B).

In a subset of the DLBCL cell lines, SEs were identified adjacent to differentially expressed genes validated as discriminating DLBCL subtypes by the COO classification (Figure S7C; Table S7). In the ABC DLBCL cell lines, but not the GCB lines, the subtype-specific TF locus *IRF4* had an adjacent SE (Figure 7A, GCB; Figure 7B, ABC; Figure 7F, tracks; Table S7). The *IRF4* SE was also detected in normal tonsil (Figure 7D), suggesting that it represented a developmental epigenetic mark rather than a tumor-specific feature. Additional genes associated with the developmental ABC signature, including *PIM1* and *CCND2*, featured adjacent SEs in ABC, but not GCB, cell lines (Figure S7C; Table S7). Observing lineage-specifying genes flanked by SEs, we explored whether SE analysis could independently discriminate DLBCL subtypes. Indeed, unsupervised bidirectional hierarchical clustering of DLBCL cell lines by SEs distinguished ABC from GCB cell lines (Figures 7I and S7C).

To evaluate the clinical significance of these findings, we performed SE analysis on primary patient samples by genome-wide ChIP-seq for H3K27ac on four primary DLBCLs that were previously subtyped as either GCB or ABC (Monti et al., 2012). All primary DLBCLs exhibited the same characteristic asymmetry in H3K27ac enrichment, with readily identified regulatory regions consistent with SEs (Figures 8A and 8B; Table S8). Again, SEs were found adjacent to lineage-specifying TFs, such as *PAX5*, and subtype-associated TFs, such as *IRF4* (Figures 8A and 8B; tracks in Figures 8C and 8D; Table S8). Importantly, aggregate unsupervised hierarchical clustering of all SE data principally segregated cell lines from primary samples (malignant or nonmalignant), whereas isolated unsupervised clustering of primary tissue segregated DLBCL samples in

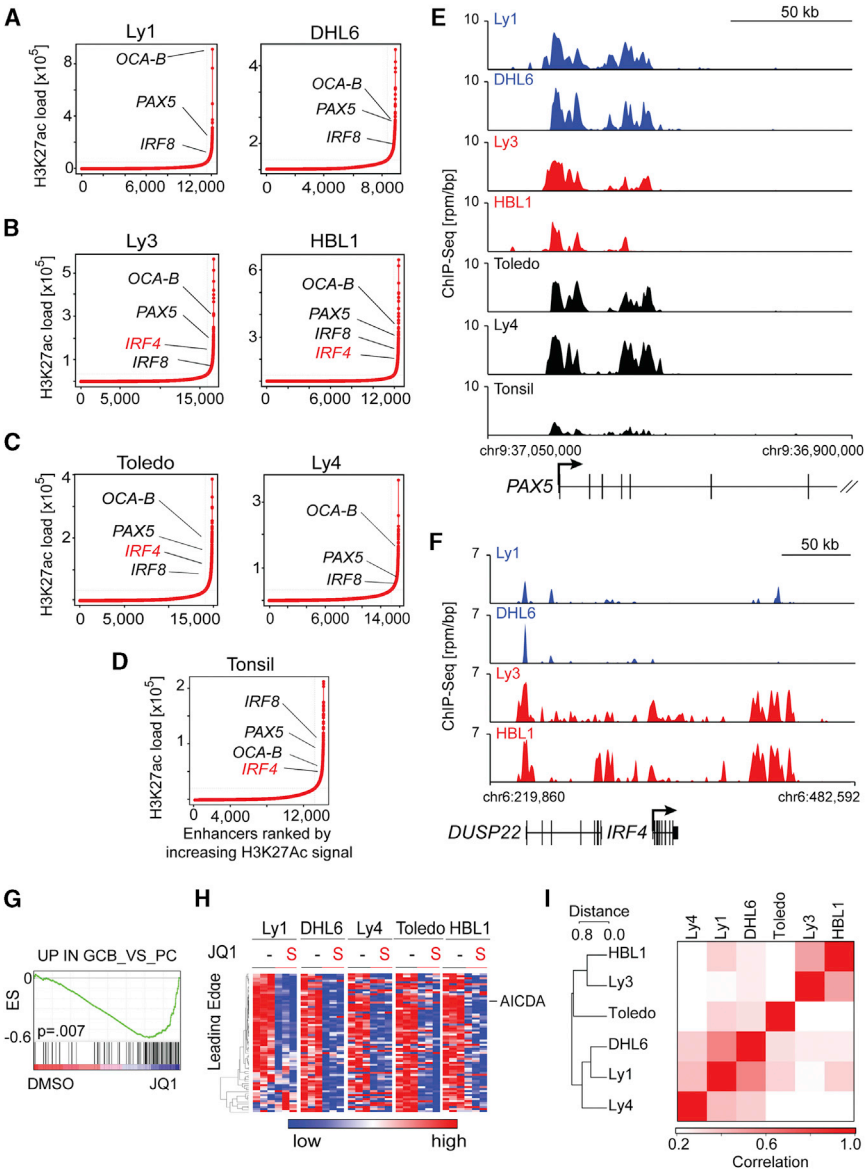

Figure 7. Comparative SE Analysis of DLBCL Cell Lines and Normal Lymphoid Tissue

(A–D) Rank order of increasing integrated H3K27ac fold enrichment at enhancer loci in DLBCL cell lines GCB (A), ABC (B), unclassified (C), and normal tonsil (D).

(E) H3K27ac ChIP-seq fold enrichment at the *PAX5* locus showing the SE region.

(F) H3K27ac ChIP-seq reads at *IRF4* locus in the two GCB and two ABC cell lines.

(G) GSEA plot of the "UP_IN GCB_VS_PC" signature in five DLBCL cell lines following JQ1 treatment.

(H) The leading edge genes of the GSEA in (G) were visualized as heatmap.

(I) Similarity matrix from unsupervised hierarchical clustering of each cell line by location of SEs.

See also Table S7 and Figure S7.

agreement with transcriptional developmental distinctions (Figures 8E and S8; Table S8).

DISCUSSION

Here, we provide mechanistic evidence of BET bromodomains as transcriptional coactivators at large enhancers and E2F1-driven promoters and contribute data supporting the study of BET inhibitors in all recognized subtypes of DLBCL. BET inhibition caused a profound G1 cell cycle arrest in a panel of DLBCL cell lines representing all transcriptionally defined subtypes and significantly delayed tumor growth in two independent DLBCL xenograft models. Gene expression profiling of multiple JQ1-treated DLBCL cell lines revealed downregulation of MYD88/TLR and BCR signaling components, which are important for certain subtypes of DLBCL (Chen et al., 2013; Ngo et al., 2011; Nicodeme et al., 2010). More broadly relevant for all subtypes of DLBCLs, we identified highly significant transcriptional downregulation of MYC and E2F1 target genes and the selective depletion of BRD4-loaded promoters and enhancers.

BET inhibition decreased the abundance of multiple functionally defined E2F target genes, but did not measurably alter E2F1 protein levels. Epigenomic analyses confirmed the colocalization of BRD4 and E2F1 at active promoters. The selective decrease in BRD4 loading of E2F1-driven genes following JQ1 treatment is consistent with studies suggesting a role of BET proteins in E2F1-mediated transcription (Peng et al., 2007; Sinha et al., 2005). Genome-wide assessment of effects of BRD4 on transcriptional elongation at E2F1 target genes was statistically significant but subtle on an individual gene level (data not shown), leaving open the possibility that BRD4-mediated effects on elongation are most apparent on SE-associated genes. Given the recently identified structural genetic signature of deregulated cell cycle and increased E2F activity in poor-prognosis DLBCLs (Monti et al., 2012), BET inhibition may represent a promising targeted treatment strategy.

Studies from our lab and others have highlighted the important role of BRD4 as a coactivator of MYC-mediated transcription (Delmore et al., 2011; Mertz et al., 2011; Ott et al., 2012). In multiple myeloma cell lines with *Ig/MYC* translocations, BRD4 was postulated to function via long-range interactions with the distal *IgH* enhancer (Delmore et al., 2011). However, emerging data indicate that BET inhibitors suppress MYC transcription in the context of translocated, amplified, or wild-type *MYC* alleles and that BRD4 localizes to *MYC* promoter and enhancer elements (Delmore et al., 2011; Lovén et al., 2013; Mertz et al., 2011; Ott et al., 2012). In the current studies, we identify a BRD4-loaded *MYC* enhancer and find that BET inhibition

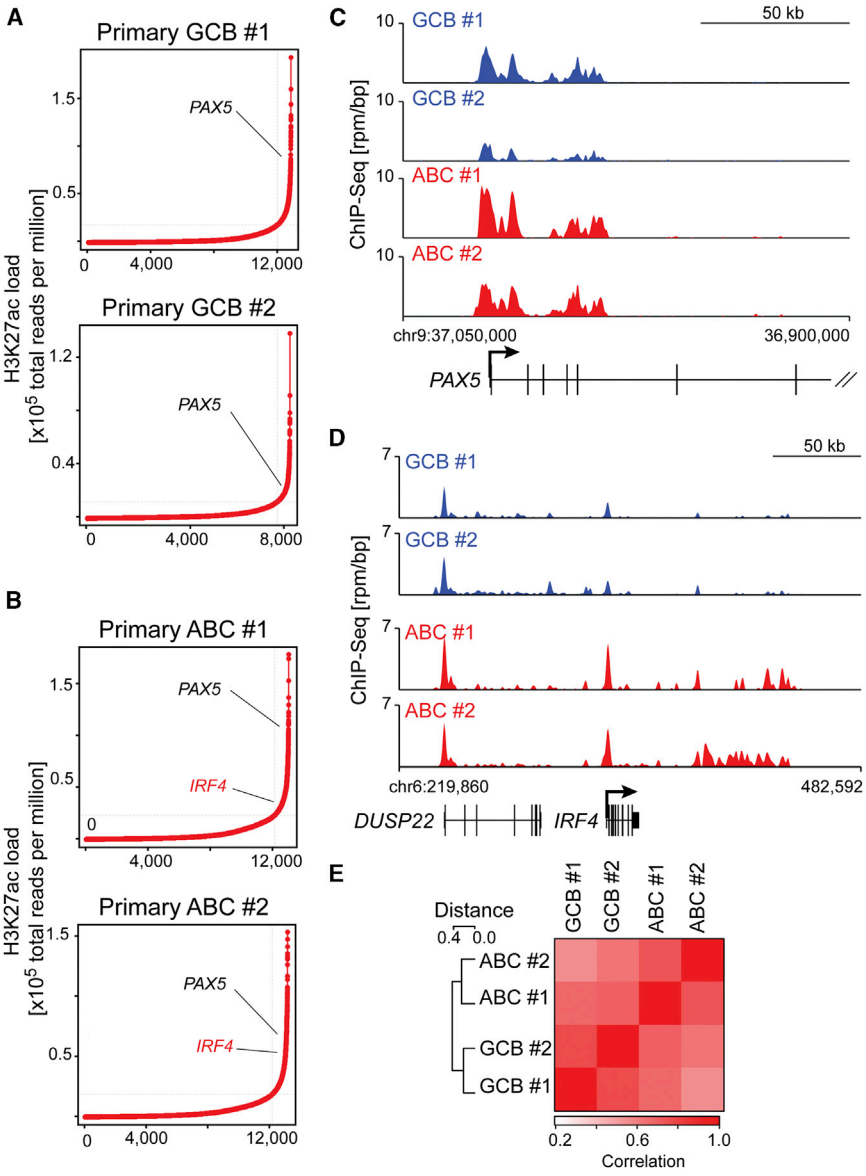

Figure 8. SE Analysis of Primary DLBCLs

(A and B) Rank order of increased H3K27ac fold enrichment at enhancer loci in primary DLBCLs: GCB#1 and #2 (A); ABC#1 and #2 (B).

(C) Gene tracks showing H3K27ac enrichment at the *PAX5* locus in all four primary DLBCLs.

(D) Tracks as in (C) comparing the H3K27 enrichment at the *IRF4* locus in primary GCB versus ABC DLBCLs.

(E) Unsupervised hierarchical clustering of primary DLBCLs using the genomic locations of all SEs in Figure S7I.

See also Table S8 and Figure S8.

decreases MYC transcription and expression in DLBCL cell lines with translocated, amplified, or wild-type MYC alleles. In this extensive DLBCL cell line panel, the functional consequences of BET inhibition—cell cycle arrest and decreased cellular proliferation—were largely comparable. Although JQ1 treatment broadly downregulated the transcriptional targets of MYC and E2F, we sought additional bases for the effect of BET inhibition across multiple DLBCL subtypes.

We observed that a small subset of genes had a disproportionately high BRD4 load at their proximal enhancers. These unusual regulatory elements were approximately 12-fold larger than typical enhancer regions. Integrated epigenomic and transcriptional studies established that such SE-marked genes were particularly sensitive to BET inhibition. As SEs were found adjacent to genes encoding known lineage factors and DLBCL oncoproteins, we surmised that SE analysis might identify previously unrecognized tumor dependencies. The functional exploration of OCA-B, encoded by SE-marked *POU2AF1*, validates this factor as a cancer dependency in DLBCL. Mechanistic research has established OCA-B as a coactivator protein that binds into the OCT1-OCT2 transcriptional complex, enhancing IgH promoter-enhancer communication (Luo and Roeder, 1995; Ren et al., 2011). Mice lacking OCA-B expression due to germline knockout of *POU2AF1* are developmentally normal, even capable of early transcription from immunoglobulin promoters; however, they lack an apparent GC reaction to antigen (Kim et al., 1996; Teitell, 2003). Collectively, the earlier studies and the current research support a putative therapeutic window to targeting OCA-B, potentially by protein-protein inhibition via the POU domain. More generally, these studies establish a rationale to systematically explore SEs for unrecognized tumor dependencies, and potentially to use SEs as biomarkers for targeted therapeutic development.

In this comparative epigenomic analysis of human DLBCL cell lines, primary tumor specimens, and normal lymphoid samples, we analyzed patterns of H3K27ac enrichment to understand the relevance of enhancer variation and function. These studies reveal SEs as characteristic features of human lymphoid tissues, both benign and malignant. Preservation of tissue-specific SEs is observed, comparing nonmalignant nodal tissue to primary DLBCL samples, as well as patient-derived human DLBCL cell lines.

In summary, our data suggest that BET inhibition limits the growth of DLBCLs by at least two complementary activities: a specific effect on genes that define a given cell type by high BRD4 loading at enhancers and a more general suppression of transcription at E2F- and MYC-driven target genes. Thus, an E2F/MYC pathway effect is combined with massive depletion of proteins driven by BRD4-overloaded enhancers, preventing cell cycle progression and leading to growth arrest. The majority of DLBCLs have a structural basis for increased E2F1-mediated

cell cycle progression; however, these tumors may differ in BRD4 super-loading of cell-fate-determining enhancers, including *MYC*, depending on their molecular context. This framework of BET inhibition explains its broad subclass- and tumor-type-independent mechanism of action and reconciles the apparent pleiotropic effects and cell type-specific outcomes. Importantly, these data provide a compelling rationale for further human clinical investigation.

EXPERIMENTAL PROCEDURES

High-Throughput Screening of BET Bromodomain Inhibitors in B Cell Lymphoma Cell Line Panel

Using a semiautomated screen, we tested the indicated compounds in 34 human lymphoma lines in a 384-well format. Cell viability at 72 hr was evaluated using ATPlite (Perkin Elmer). The means of absolute effective concentration of 50% impact (EC_{50}) from two independent screens were visualized and clustered using GENE-E (http://www.broadinstitute.org/cancer/software/GENE-E/index.html).

Human Samples

Frozen biopsy specimens of newly diagnosed, previously untreated primary DLBCLs with >80% tumor involvement and known transcriptional subtyping (Monti et al., 2012) were obtained according to Institutional Review Board (IRB)-approved protocols (Brigham and Women's Hospital and Dana-Farber Cancer Institute). A waiver to obtain informed consent was granted by the local IRBs because only coded, deidentified, discarded tissue was used.

Animal Studies

All animal studies were performed according to Dana-Farber Cancer Institute Institutional Animal Care and Use Committee-approved protocols, as previously described (Monti et al., 2012), and Supplemental Experimental Procedures.

Analyses of Cellular Proliferation and Apoptosis, Immunohistochemistry, Immunoblotting, Transcriptional Profiling, GSEA and Lentiviral-Mediated shRNA, ChIP-Seq, and Analysis of ChIP-Seq Data

A full description of these methods is listed in Supplemental Experimental Procedures.

ACCESSION NUMBERS

The Gene Expression Omnibus accession numbers for the gene expression and ChIP-seq data reported in this paper are GSE45630 and GSE46663, respectively.

SUPPLEMENTAL INFORMATION

Supplemental Information includes Supplemental Experimental Procedures, eight figures, and eight tables and can be found with this article online at http://dx.doi.org/10.1016/j.ccr.2013.11.003.

ACKNOWLEDGMENTS

The authors acknowledge support from the National Institutes of Health and the Leukemia & Lymphoma Society (to M.A.S. and J.E.B.); the Damon-Runyon Cancer Research Foundation, the Broad New Idea Award, the William Lawrence and Blanche Hughes Foundation; and the American Society of Hematology (to J.E.B.); the Department of Defense (CDMRP CA120184 to C.Y.L.); the American Cancer Society (PF-11-042-01-DMC to P.B.R.); and the German Research Foundation (DFG Ch 735/1-1 to B.C.). Drug-like derivities of JQ1 have been licensed to Tensha Therapuetics for clinical development by DFCI. J.E.B. is a Scientific Founder of Tensha. J.E.B. and R.A.Y. are Scientific Founders of Syros Pharmacueticals. C.Y.L. and P.B.R. were paid consultants for Syros Pharmaceuticals.

Received: May 24, 2013
Revised: September 17, 2013
Accepted: November 6, 2013
Published: December 9, 2013

REFERENCES

Bartholomeeusen, K., Xiang, Y., Fujinaga, K., and Peterlin, B.M. (2012). Bromodomain and extra-terminal (BET) bromodomain inhibition activate transcription via transient release of positive transcription elongation factor b (P-TEFb) from 7SK small nuclear ribonucleoprotein. J. Biol. Chem. *287*, 36609–36616.

Basso, K., and Dalla-Favera, R. (2012). Roles of BCL6 in normal and transformed germinal center B cells. Immunol. Rev. *247*, 172–183.

Bisgrove, D.A., Mahmoudi, T., Henklein, P., and Verdin, E. (2007). Conserved P-TEFb-interacting domain of BRD4 inhibits HIV transcription. Proc. Natl. Acad. Sci. USA *104*, 13690–13695.

Caro, P., Kishan, A.U., Norberg, E., Stanley, I.A., Chapuy, B., Ficarro, S.B., Polak, K., Tondera, D., Gounarides, J., Yin, H., et al. (2012). Metabolic signatures uncover distinct targets in molecular subsets of diffuse large B cell lymphoma. Cancer Cell *22*, 547–560.

Chen, L., Monti, S., Juszczynski, P., Ouyang, J., Chapuy, B., Neuberg, D., Doench, J.G., Bogusz, A.M., Habermann, T.M., Dogan, A., et al. (2013). SYK inhibition modulates distinct PI3K/AKT-dependent survival pathways and cholesterol biosynthesis in diffuse large B cell lymphomas. Cancer Cell *23*, 826–838.

Cobaleda, C., Schebesta, A., Delogu, A., and Busslinger, M. (2007). Pax5: the guardian of B cell identity and function. Nat. Immunol. *8*, 463–470.

Dawson, M.A., Prinjha, R.K., Dittmann, A., Giotopoulos, G., Bantscheff, M., Chan, W.I., Robson, S.C., Chung, C.W., Hopf, C., Savitski, M.M., et al. (2011). Inhibition of BET recruitment to chromatin as an effective treatment for MLL-fusion leukaemia. Nature *478*, 529–533.

Delmore, J.E., Issa, G.C., Lemieux, M.E., Rahl, P.B., Shi, J., Jacobs, H.M., Kastritis, E., Gilpatrick, T., Paranal, R.M., Qi, J., et al. (2011). BET bromodomain inhibition as a therapeutic strategy to target c-Myc. Cell *146*, 904–917.

Dey, A., Chitsaz, F., Abbasi, A., Misteli, T., and Ozato, K. (2003). The double bromodomain protein Brd4 binds to acetylated chromatin during interphase and mitosis. Proc. Natl. Acad. Sci. USA *100*, 8758–8763.

Filippakopoulos, P., Qi, J., Picaud, S., Shen, Y., Smith, W.B., Fedorov, O., Morse, E.M., Keates, T., Hickman, T.T., Felletar, I., et al. (2010). Selective inhibition of BET bromodomains. Nature *468*, 1067–1073.

Filippakopoulos, P., Picaud, S., Mangos, M., Keates, T., Lambert, J.P., Barsyte-Lovejoy, D., Felletar, I., Volkmer, R., Müller, S., Pawson, T., et al. (2012). Histone recognition and large-scale structural analysis of the human bromodomain family. Cell *149*, 214–231.

Fuda, N.J., Ardehali, M.B., and Lis, J.T. (2009). Defining mechanisms that regulate RNA polymerase II transcription in vivo. Nature *461*, 186–192.

Gisselbrecht, C., Glass, B., Mounier, N., Singh Gill, D., Linch, D.C., Trneny, M., Bosly, A., Ketterer, N., Shpilberg, O., Hagberg, H., et al. (2010). Salvage regimens with autologous transplantation for relapsed large B-cell lymphoma in the rituximab era. J. Clin. Oncol. *28*, 4184–4190.

Greenwald, R.J., Tumang, J.R., Sinha, A., Currier, N., Cardiff, R.D., Rothstein, T.L., Faller, D.V., and Denis, G.V. (2004). E mu-BRD2 transgenic mice develop B-cell lymphoma and leukemia. Blood *103*, 1475–1484.

Greiner, A., Müller, K.B., Hess, J., Pfeffer, K., Müller-Hermelink, H.K., and Wirth, T. (2000). Up-regulation of BOB.1/OBF.1 expression in normal germinal center B cells and germinal center-derived lymphomas. Am. J. Pathol. *156*, 501–507.

Hu, S., Xu-Monette, Z.Y., Tzankov, A., Green, T., Wu, L., Balasubramanyam, A., Liu, W.M., Visco, C., Li, Y., Miranda, R.N., et al. (2013). MYC/BCL2 protein coexpression contributes to the inferior survival of activated B-cell subtype of diffuse large B-cell lymphoma and demonstrates high-risk gene expression signatures: a report from The International DLBCL Rituximab-CHOP Consortium Program. Blood *121*, 4021–4031, quiz 4250.

Johnson, N.A., Slack, G.W., Savage, K.J., Connors, J.M., Ben-Neriah, S., Rogic, S., Scott, D.W., Tan, K.L., Steidl, C., Sehn, L.H., et al. (2012). Concurrent expression of MYC and BCL2 in diffuse large B-cell lymphoma treated with rituximab plus cyclophosphamide, doxorubicin, vincristine, and prednisone. J. Clin. Oncol. *30*, 3452–3459.

Kim, U., Qin, X.F., Gong, S., Stevens, S., Luo, Y., Nussenzweig, M., and Roeder, R.G. (1996). The B-cell-specific transcription coactivator OCA-B/OBF-1/Bob-1 is essential for normal production of immunoglobulin isotypes. Nature *383*, 542–547.

Klein, U., and Dalla-Favera, R. (2008). Germinal centres: role in B-cell physiology and malignancy. Nat. Rev. Immunol. *8*, 22–33.

Lee, T.I., and Young, R.A. (2013). Transcriptional regulation and its misregulation in disease. Cell *152*, 1237–1251.

Lenz, G., and Staudt, L.M. (2010). Aggressive lymphomas. N. Engl. J. Med. *362*, 1417–1429.

Lohr, J.G., Stojanov, P., Lawrence, M.S., Auclair, D., Chapuy, B., Sougnez, C., Cruz-Gordillo, P., Knoechel, B., Asmann, Y.W., Slager, S.L., et al. (2012). Discovery and prioritization of somatic mutations in diffuse large B-cell lymphoma (DLBCL) by whole-exome sequencing. Proc. Natl. Acad. Sci. USA *109*, 3879–3884.

Lovén, J., Hoke, H.A., Lin, C.Y., Lau, A., Orlando, D.A., Vakoc, C.R., Bradner, J.E., Lee, T.I., and Young, R.A. (2013). Selective inhibition of tumor oncogenes by disruption of super-enhancers. Cell *153*, 320–334.

Luo, Y., and Roeder, R.G. (1995). Cloning, functional characterization, and mechanism of action of the B-cell-specific transcriptional coactivator OCA-B. Mol. Cell. Biol. *15*, 4115–4124.

Marushige, K. (1976). Activation of chromatin by acetylation of histone side chains. Proc. Natl. Acad. Sci. USA *73*, 3937–3941.

Mertz, J.A., Conery, A.R., Bryant, B.M., Sandy, P., Balasubramanian, S., Mele, D.A., Bergeron, L., and Sims, R.J., 3rd. (2011). Targeting MYC dependence in cancer by inhibiting BET bromodomains. Proc. Natl. Acad. Sci. USA *108*, 16669–16674.

Miyoshi, S., Ooike, S., Iwata, K., Hikawa, H., and Sugaraha, K. September 2009. Antitumor agent. International patent PCT/JP2008/073864 (WO/2009/084693).

Monti, S., Savage, K.J., Kutok, J.L., Feuerhake, F., Kurtin, P., Mihm, M., Wu, B., Pasqualucci, L., Neuberg, D., Aguiar, R.C., et al. (2005). Molecular profiling of diffuse large B-cell lymphoma identifies robust subtypes including one characterized by host inflammatory response. Blood *105*, 1851–1861.

Monti, S., Chapuy, B., Takeyama, K., Rodig, S.J., Hao, Y., Yeda, K.T., Inguilizian, H., Mermel, C., Currie, T., Dogan, A., et al. (2012). Integrative analysis reveals an outcome-associated and targetable pattern of p53 and cell cycle deregulation in diffuse large B cell lymphoma. Cancer Cell *22*, 359–372.

Morin, R.D., Mendez-Lago, M., Mungall, A.J., Goya, R., Mungall, K.L., Corbett, R.D., Johnson, N.A., Severson, T.M., Chiu, R., Field, M., et al. (2011). Frequent mutation of histone-modifying genes in non-Hodgkin lymphoma. Nature *476*, 298–303.

Ngo, V.N., Young, R.M., Schmitz, R., Jhavar, S., Xiao, W., Lim, K.H., Kohlhammer, H., Xu, W., Yang, Y., Zhao, H., et al. (2011). Oncogenically active MYD88 mutations in human lymphoma. Nature *470*, 115–119.

Nicodeme, E., Jeffrey, K.L., Schaefer, U., Beinke, S., Dewell, S., Chung, C.W., Chandwani, R., Marazzi, I., Wilson, P., Coste, H., et al. (2010). Suppression of inflammation by a synthetic histone mimic. Nature *468*, 1119–1123.

Nutt, S.L., Taubenheim, N., Hasbold, J., Corcoran, L.M., and Hodgkin, P.D. (2011). The genetic network controlling plasma cell differentiation. Semin. Immunol. *23*, 341–349.

Ott, C.J., Kopp, N., Bird, L., Paranal, R.M., Qi, J., Bowman, T., Rodig, S.J., Kung, A.L., Bradner, J.E., and Weinstock, D.M. (2012). BET bromodomain inhibition targets both c-Myc and IL7R in high-risk acute lymphoblastic leukemia. Blood *120*, 2843–2852.

Owen, D.J., Ornaghi, P., Yang, J.C., Lowe, N., Evans, P.R., Ballario, P., Neuhaus, D., Filetici, P., and Travers, A.A. (2000). The structural basis for the recognition of acetylated histone H4 by the bromodomain of histone acetyltransferase gcn5p. EMBO J. *19*, 6141–6149.

Pasqualucci, L., Trifonov, V., Fabbri, G., Ma, J., Rossi, D., Chiarenza, A., Wells, V.A., Grunn, A., Messina, M., Elliot, O., et al. (2011). Analysis of the coding genome of diffuse large B-cell lymphoma. Nat. Genet. *43*, 830–837.

Peng, J., Dong, W., Chen, L., Zou, T., Qi, Y., and Liu, Y. (2007). Brd2 is a TBP-associated protein and recruits TBP into E2F-1 transcriptional complex in response to serum stimulation. Mol. Cell. Biochem. *294*, 45–54.

Polo, J.M., Juszczynski, P., Monti, S., Cerchietti, L., Ye, K., Greally, J.M., Shipp, M., and Melnick, A. (2007). Transcriptional signature with differential expression of BCL6 target genes accurately identifies BCL6-dependent diffuse large B cell lymphomas. Proc. Natl. Acad. Sci. USA *104*, 3207–3212.

Puissant, A., Frumm, S.M., Alexe, G., Bassil, C.F., Qi, J., Chanthery, Y.H., Nekritz, E.A., Zeid, R., Gustafson, W.C., Greninger, P., et al. (2013). Targeting MYCN in neuroblastoma by BET bromodomain inhibition. Cancer Discov. *3*, 308–323.

Ramachandrareddy, H., Bouska, A., Shen, Y., Ji, M., Rizzino, A., Chan, W.C., and McKeithan, T.W. (2010). BCL6 promoter interacts with far upstream sequences with greatly enhanced activating histone modifications in germinal center B cells. Proc. Natl. Acad. Sci. USA *107*, 11930–11935.

Ren, X., Siegel, R., Kim, U., and Roeder, R.G. (2011). Direct interactions of OCA-B and TFII-I regulate immunoglobulin heavy-chain gene transcription by facilitating enhancer-promoter communication. Mol. Cell *42*, 342–355.

Schreiber, S.L., and Bernstein, B.E. (2002). Signaling network model of chromatin. Cell *111*, 771–778.

Sinha, A., Faller, D.V., and Denis, G.V. (2005). Bromodomain analysis of Brd2-dependent transcriptional activation of cyclin A. Biochem. J. *387*, 257–269.

Slack, G.W., and Gascoyne, R.D. (2011). MYC and aggressive B-cell lymphomas. Adv. Anat. Pathol. *18*, 219–228.

Teitell, M.A. (2003). OCA-B regulation of B-cell development and function. Trends Immunol. *24*, 546–553.

Wang, H., Lee, C.H., Qi, C., Tailor, P., Feng, J., Abbasi, S., Atsumi, T., and Morse, H.C., 3rd. (2008). IRF8 regulates B-cell lineage specification, commitment, and differentiation. Blood *112*, 4028–4038.

Yang, Z., He, N., and Zhou, Q. (2008). Brd4 recruits P-TEFb to chromosomes at late mitosis to promote G1 gene expression and cell cycle progression. Mol. Cell. Biol. *28*, 967–976.

Ye, B.H., Cattoretti, G., Shen, Q., Zhang, J., Hawe, N., de Waard, R., Leung, C., Nouri-Shirazi, M., Orazi, A., Chaganti, R.S., et al. (1997). The BCL-6 proto-oncogene controls germinal-centre formation and Th2-type inflammation. Nat. Genet. *16*, 161–170.

Zhang, W., Prakash, C., Sum, C., Gong, Y., Li, Y., Kwok, J.J., Thiessen, N., Pettersson, S., Jones, S.J., Knapp, S., et al. (2012). Bromodomain-containing protein 4 (BRD4) regulates RNA polymerase II serine 2 phosphorylation in human CD4+ T cells. J. Biol. Chem. *287*, 43137–43155.

Zhang, J., Grubor, V., Love, C.L., Banerjee, A., Richards, K.L., Mieczkowski, P.A., Dunphy, C., Choi, W., Au, W.Y., Srivastava, G., et al. (2013). Genetic heterogeneity of diffuse large B-cell lymphoma. Proc. Natl. Acad. Sci. USA *110*, 1398–1403.

Zhao, R., Nakamura, T., Fu, Y., Lazar, Z., and Spector, D.L. (2011). Gene bookmarking accelerates the kinetics of post-mitotic transcriptional re-activation. Nat. Cell Biol. *13*, 1295–1304.

Zuber, J., Shi, J., Wang, E., Rappaport, A.R., Herrmann, H., Sison, E.A., Magoon, D., Qi, J., Blatt, K., Wunderlich, M., et al. (2011). RNAi screen identifies Brd4 as a therapeutic target in acute myeloid leukaemia. Nature *478*, 524–528.